

# Supporting Information

## Implementation of trait-based ozone plant sensitivity in the Yale Interactive terrestrial Biosphere model v1.0 to assess global vegetation damage

Yimian Ma<sup>1,2</sup>, Xu Yue<sup>3\*</sup>, Stephen Sitch<sup>4\*</sup>, Nadine Unger<sup>3</sup>, Johan Uddling<sup>5</sup>, Lina M. Mercado<sup>4,6</sup>, Cheng Gong<sup>7</sup>, Zhaozhong Feng<sup>8</sup>, Huiyi Yang<sup>9</sup>, Hao Zhou<sup>1,2</sup>, Chenguang Tian<sup>1,2</sup>, Yang Cao<sup>1,2</sup>, Yadong Lei<sup>10</sup>, Alexander W. Cheesman<sup>4,11</sup>, Yansen Xu<sup>8</sup>, Maria Carolina Duran Rojas<sup>12</sup>

<sup>1</sup> Climate Change Research Center, Institute of Atmospheric Physics, Chinese Academy of Sciences, Beijing, 100029, China

<sup>2</sup> University of Chinese Academy of Sciences, Beijing, 100029, China

<sup>3</sup> Jiangsu Key Laboratory of Atmospheric Environment Monitoring and Pollution Control, Jiangsu Collaborative Innovation Center of Atmospheric Environment and Equipment Technology, School of Environmental Science and Engineering, Nanjing University of Information Science and Technology, Nanjing, 210044, China

<sup>4</sup> Faculty of Environment, Science and Economy, University of Exeter, Exeter, EX4 4RJ, UK

<sup>5</sup> Department of Biological and Environmental Sciences, University of Gothenburg, Gothenburg, P.O. Box 461, 40530, Sweden

<sup>6</sup> UK Centre for Ecology and Hydrology, Benson Lane, Wallingford, OX10 8BB, UK

<sup>7</sup> State Key Laboratory of Atmospheric Boundary Layer Physics and Atmospheric Chemistry (LAPC), Institute of Atmospheric Physics, Chinese Academy of Sciences, Beijing, 100029, China

<sup>8</sup> School of Applied Meteorology, Nanjing University of Information Science and Technology, Nanjing, 210044, China

<sup>9</sup> Livelihoods and Institutions Department, Natural Resources Institute, University of Greenwich, Kent, ME4 4TB, UK

<sup>10</sup> Chinese Academy of Meteorological Sciences, Beijing, 100081, China

<sup>11</sup> Centre for Tropical Environmental and Sustainability Science, College of Science & Engineering, James Cook University, Cairns, Queensland, 4870 Australia

<sup>12</sup> College of Engineering, Mathematics, and Physical Sciences, University of Exeter, Exeter, EX4 4PY, UK

36 **Table S1.** Data for calibration. Each  $S_O$  (% per  $\text{mmol m}^{-2}$ ) value is derived as the slope of regression  
 37 between the corresponding  $O_3$  metric ( $\phi_{O_3}$ ) and relative bio-indicator ( $R$ ) in Equation (5).

38

PFT	Reference	Species	Regions	$\phi_{O_3}$	$D$	$S_O$	Sub-references
EBF (median $S_O$ : -0.19)	Clrtap (2017) Figure III.12	Quercus ilex L.	Spain	POD <sub>y=1</sub>	Above-ground biomass	-0.09	Alonso et al. (2014)
	Assis et al. (2015)	Psidium guajava L. 'Paluma'	Brazil	POD <sub>y=1</sub>	Leaf injury index	-0.19 -0.05 -0.2 -0.58	
NF (median $S_O$ : -0.23)	Clrtap (2017) Figure III.12	Picea abies	France, Sweden, Switzerland and	POD <sub>y=1</sub>	Total biomass	-0.22	Buker et al. (2015)
	Feng et al. (2018)	Picea abies, Pinus halepensis, Pinus sylvestris	Europe	POD <sub>y=1</sub>	Total biomass	-0.24	Elvira et al. (2007); Karlsson et al. (2004); Ottosson et al. (2003); Alonso et al. (2003); Medlyn et al. (1999); Braun and Fluckiger (1995)
DBF (median $S_O$ : -0.70)	Clrtap (2017) Figure III.12	Fagus sylvatica, Betula pendula	Finland, Sweden, Switzerland and	POD <sub>y=1</sub>	Total biomass	-0.93	Buker et al. (2015)
	Clrtap (2017) Figure III.12	Quercus faginea; Q. pyrenaica, Q. robur	Italy, Spain	POD <sub>y=1</sub>	Total biomass	-0.32	Calatayud et al. (2011); Marzuoli et al. (2016)
	Buker et al. (2015) Supplementary data	Betula pendula Quercus robur	Europe	POD <sub>y=1</sub>	Total biomass	-0.61	Uddling et al. (2004); Ottosson et al. (2003); Dixon et al. (1998); Karlsson et al. (2003)
	Hoshika et al. (2018)	Quercus pubescens, Q. robur	Italy	POD <sub>y=1</sub>	Total biomass	-0.73, -1.4	
	Marzuoli et al. (2018)	Quercus pyrenaica, Q. faginea, Q. robur	Spain, Italy	POD <sub>y=1</sub> POD <sub>y=1</sub>	Total biomass Total biomass	-0.32, -0.52	
	Hu et al. (2015)	Poplar (5 clones)	China	POD <sub>y=1</sub>	Total biomass	-0.75	
GRA_C4 (median $S_O$ : -0.85)	Clrtap (2017) Figure III.14	Mediterranean pasture	Spain	POD <sub>y=1</sub>	Above-ground biomass	-0.85	Gimeno et al. (2004a); Gimeno et al. (2004b); Sanz et al. (2005); Sanz et al. (2007); Sanz

GRA_C3 (median $S_O$ : -0.62)	Clrtap (2017) Figure III.13	Temperate grassland	UK	POD <sub>y=1</sub>	Total biomass	-0.62	et al. (2014); Sanz et al. (2016) Hayes et al. (2011); Hayes et al. (2012) Wyness et al. (2011); Wagg et al. (2012); Hewitt et al. (2014)
CRO (median $S_O$ : -3.35)	Peng et al. (2020)	Maize (2 varieties)	China	POD <sub>y=6</sub>	Total biomass	-5.26	
	Peng et al. (2019)	Maize	China	POD <sub>y=6</sub>	Total biomass	-4.26	
	Hayes et al. (2020)	Bean, Cowpea (13 varieties)	Africa	POD <sub>y=6</sub>	Yield	-2.58	
				POD <sub>y=6</sub>	Thousa nd grain weight	-1.2	
	Hayes et al. (2020)	Wheat	Africa	POD <sub>y=6</sub>	Yield	-3.5	
				POD <sub>y=6</sub>	Thousa nd grain weight	-2.9	
	Clrtap (2017) Figure III.10	Wheat	Synthesi s	POD <sub>y=6</sub>	Grain yield	-3.85	
	Clrtap (2017) Figure III.10	Wheat	Synthesi s	POD <sub>y=6</sub>	1000 grain yield	-3.35	
	Clrtap (2017) Figure III.10	Wheat	Synthesi s	POD <sub>y=6</sub>	Protein producti on	-2.54	
	Clrtap (2017) Figure III.11	Tomato	Synthesi s	POD <sub>y=6</sub>	Yield	-2.53	
Clrtap (2017) Table III.10	Tomato	Synthesi s	POD <sub>y=6</sub>	Fruit yield	-2.66		
Zhang et al. (2017)	Soybean	China	POD <sub>y=6</sub>	Seed yield	-3.3		
Harmens et al. (2018)	Wheat (2 varieties)	Europe	POD <sub>y=6</sub>	Yield	-3.9		
			POD <sub>y=6</sub>	Yield	-6.5		
			POD <sub>y=6</sub>	1000	-3.4		
			POD <sub>y=6</sub>	grain weight	-4.8		
				1000 grain weight			

39

40

41 **Table S2.** PFT-specific LMA for the YIBs-LMA\_PFT<sup>a</sup> experiment.

42

PFT	EBF	NF	DBF	C_SHR	A_SHR	C4_GRA	C3_GRA	CRO
LMA <sup>b</sup> (g m <sup>-2</sup> )	83.9	158.1	53.9	68.8	68.8	47.7	47.7	47.7
Source types <sup>c</sup>	EBF	ENF, DNF	DBF	SHL	SHL	GRL	GRL	GRL

43

44 <sup>a</sup> The YIBs-LMA\_PFT experiment uses  $x=0.019$  nmol g<sup>-1</sup> s<sup>-1</sup> and PFT-specific LMA from M2018,  
 45 which is different from YIBs-LMA in the way of LMA assignment. Details are summarized in  
 46 Table 1.

47 <sup>b</sup> The average LMA for certain PFT is calculated from M2018 dataset.

48 <sup>c</sup> For each PFT in the YIBs model, the vegetation types from original paper of M2018 are listed,  
 49 including EBF, ENF, DNF (Deciduous needleleaf forest), DBF, SHL (shrubland), and GRL  
 50 (grassland).

51

52 **Table S3.** Calibrations of the YIBs-LMA <sup>a</sup> experiment with varied  $a$ .

53

PFT	$S_O$						$S_S/S_O$ <sup>b</sup>				
		a=2.5	a=3.0	<b>a=3.5</b>	a=4.0	a=4.5	a=2.5	a=3.0	<b>a=3.5</b>	a=4.0	a=4.5
EBF	-0.19	-0.13	-0.16	<b>-0.18</b>	-0.21	-0.23	0.70	0.83	<b>0.96</b>	1.08	1.20
NF	-0.23	-0.26	-0.31	<b>-0.36</b>	-0.40	-0.45	1.14 *	1.35 *	<b>1.56 *</b>	1.75 *	1.95 *
DBF	-0.70	-0.51	-0.60	<b>-0.69</b>	-0.78	-0.87	0.72	0.86	<b>0.99</b>	1.12	1.24
C_SHR	/	-0.75	-0.90	<b>-1.04</b>	-1.18	-1.31	/	/	/	/	/
A_SHR	/	-0.38	-0.45	<b>-0.53</b>	-0.60	-0.66	/	/	/	/	/
C4_GRA	-0.85	-0.71	-0.84	<b>-0.97</b>	-1.10	-1.22	0.83	0.99	<b>1.14</b>	1.29	1.44
C3_GRA	-0.62	-0.47	-0.55	<b>-0.64</b>	-0.73	-0.81	0.75	0.89	<b>1.03</b>	1.17	1.30
CRO	-3.35	-1.97	-2.57	<b>-3.28</b>	-4.11	-5.10	0.59	0.77	<b>0.98</b>	1.23	1.52
Fitting <sup>c</sup>	/	0.61	0.79	<b>0.99</b>	1.23	1.50	/	/	/	/	/
Median	/	/	/	/	/	/	0.74 (0.72)	0.88 (0.86)	<b>1.01</b> ( <b>0.99</b> )	1.20 (1.17)	1.37 (1.30)
Std	/	/	/	/	/	/	0.19 (0.09)	0.21 (0.08)	<b>0.23</b> ( <b>0.07</b> )	0.25 (0.08)	0.28 (0.13)

54

55 <sup>a</sup> All runs from the YIBs-LMA experiment use  $x=0.019$  nmol g<sup>-1</sup> s<sup>-1</sup> and LMA map from M2018.  
 56 Details are summarized in Table 1.

57 <sup>b</sup> Slopes of simulated DRRs ( $S_S$ ) are divided by observations ( $S_O$ , Table S1) to derive the model-to-  
 58 observation ratios (“ $S_S/S_O$ ”). O<sub>3</sub> dose metric is POD<sub>y=1</sub> for natural PFTs and POD<sub>y=6</sub> for crops. The  
 59 Median and standard deviation (Std) of  $S_S/S_O$  ratios of all PFTs are calculated for each set of specific  
 60 parameter  $a$ . The values in parentheses exclude the effect of those numbers marked with \* that are  
 61 out of 1 standard deviation.

62 <sup>c</sup> The slopes (Fitting) of linear regressions between  $S_O$  and  $S_S$  are listed for each  $a$ . The optimal  $a$   
 63 with 1:1 fitting between  $S_S$  and  $S_O$  is bolded.

64

65 **Table S4.** Calibrations of the YIBs-LMA\_PFT <sup>a</sup> experiment with varied *a*.

66

PFT	$S_O$	$S_S$					$S_S/S_O$ <sup>b</sup>				
		a=2.0	a=2.5	a=3.0	a=3.5	a=4.0	a=2.0	a=2.5	a=3.0	a=3.5	a=4.0
EBF	-0.19	<b>-0.14</b>	-0.18	-0.21	-0.25	-0.28	<b>0.76</b>	0.95	1.13	1.30	1.48
NF	-0.23	<b>-0.07</b>	-0.09	-0.11	-0.12	-0.14	<b>0.32 *</b>	0.4 *	0.47 *	0.54 *	0.61 *
DBF	-0.70	<b>-0.63</b>	-0.78	-0.92	-1.07	-1.21	<b>0.90</b>	1.11	1.32	1.53	1.73
C_SHR	/	<b>-0.72</b>	-0.90	-1.07	-1.24	-1.41	/	/	/	/	/
A_SHR	/	<b>-0.39</b>	-0.48	-0.58	-0.67	-0.76	/	/	/	/	/
C4_GRA	-0.85	<b>-0.92</b>	-1.15	-1.37	-1.59	-1.81	<b>1.09</b>	1.35	1.61	1.87	2.13
C3_GRA	-0.62	<b>-0.68</b>	-0.84	-1.00	-1.17	-1.33	<b>1.09</b>	1.36	1.62	1.88	2.14
CRO	-3.35	<b>-3.34</b>	-5.05	-7.51	-11.21	-17.08	<b>1.00</b>	1.51	2.24	3.35	5.10
Fitting <sup>c</sup>	/	<b>1.00</b>	1.47	2.14	3.13	4.69	/	/	/	/	/
Median	/	/	/	/	/	/	<b>0.95</b> <b>(1.00)</b>	1.23 (1.35)	1.47 (1.61)	1.70 (1.87)	1.93 (2.13)
Std	/	/	/	/	/	/	<b>0.29</b> <b>(0.14)</b>	0.4 (0.22)	0.59 (0.42)	0.93 (0.80)	1.53 (1.47)

67

68 <sup>a</sup> All tests of the YIBs-LMA\_PFT experiment use  $x=0.019$  nmol g<sup>-1</sup> s<sup>-1</sup> and PFT-specific LMA  
69 information from M2018 (Table S2), which is different from YIBs-LMA in the way of LMA  
70 assignment.

71 <sup>b</sup> Slopes of simulated PFT-specific DRRs ( $S_S$ ) are divided by observations ( $S_O$ , Table S1) to derive  
72 the model-to-observation ratios ( $S_S/S_O$ ). O<sub>3</sub> dose metric is POD<sub>y=1</sub> for natural PFTs and POD<sub>y=6</sub> for  
73 crops. The Median and standard deviation (Std) of  $S_S/S_O$  ratios of all PFTs are calculated for each  
74 set of specific parameter *a*. The values in parentheses exclude the effect of those numbers marked  
75 with \* that are out of 1 standard deviation.

76 <sup>c</sup> The slopes (Fitting) of linear regressions between  $S_O$  and  $S_S$  are listed for each *a*. The optimal *a*  
77 with 1:1 fitting between  $S_S$  and  $S_O$  is bolded.

78

79 **Table S5.** Calibrations of the YIBs-LMA\_T <sup>a</sup> experiment with varied *a*.

80

PFT	$S_O$	$S_S$					$S_S/S_O$ <sup>b</sup>				
		a=2.0	a=2.5	<b>a=3.0</b>	a=3.5	a=4.0	a=2.0	a=2.5	<b>a=3.0</b>	a=3.5	a=4.0
EBF	-0.19	-0.21	-0.26	<b>-0.31</b>	-0.36	-0.41	1.08	1.35	<b>1.62</b>	1.89	2.16
NF	-0.23	-0.33	-0.41	<b>-0.49</b>	-0.57	-0.65	1.43	1.78	<b>2.14</b>	2.49	2.84
DBF	-0.70	-0.50	-0.63	<b>-0.75</b>	-0.87	-0.99	0.72	0.90	<b>1.07</b>	1.25	1.42
C_SHR	/	-1.10	-1.38	<b>-1.66</b>	-1.94	-2.23	/	/	/	/	/
A_SHR	/	-0.44	-0.55	<b>-0.67</b>	-0.78	-0.89	/	/	/	/	/
C4_GRA	-0.85	-0.87	-1.09	<b>-1.31</b>	-1.53	-1.76	1.02	1.28	<b>1.54</b>	1.80	2.07
C3_GRA	-0.62	-0.49	-0.61	<b>-0.73</b>	-0.85	-0.98	0.79	0.98	<b>1.18</b>	1.38	1.57
CRO	-3.35	-1.72	-2.38	<b>-3.19</b>	-4.19	-5.43	0.51	0.71	<b>0.95</b>	1.25	1.62
Fitting <sup>c</sup>	/	0.56	0.76	<b>1.00</b>	1.29	1.64	/	/	/	/	/
Median	/	/	/	/	/	/	0.91	1.13	<b>1.36</b>	1.59	1.84
Std	/	/	/	/	/	/	0.32	0.39	<b>0.44</b>	0.49	0.53

81

82 <sup>a</sup> All tests from the YIBs-LMA\_T experiment use the threshold  $x=0.006 \text{ nmol g}^{-1} \text{ s}^{-1}$  and the gridded  
 83 LMA from of M2018 map. Details are summarized in Table 1.

84 <sup>b</sup> Slopes of simulated PFT-specific DRR ( $S_S$ ) are divided by observations ( $S_O$ , Table S1) to derive  
 85 the model-to-observation ratios ( $S_S/S_O$ ).  $O_3$  dose metric is  $POD_{y=1}$  for natural PFTs and  $POD_{y=6}$  for  
 86 crops. The Median and standard deviation (Std) of  $S_S/S_O$  ratios of all PFTs are calculated for each  
 87 set of specific parameter *a*.

88 <sup>c</sup> The slopes (Fitting) of linear regressions between  $S_O$  and  $S_S$  are listed for each *a*. The optimal *a*  
 89 with 1:1 fitting between  $S_S$  and  $S_O$  is bolded.

90

91 **Table S6.** Calibrations of the YIBs-LMA\_B2017<sup>a</sup> experiment with varied  $a$ .

92

PFT	$S_O$	$S_S$					$S_S/S_O$ <sup>b</sup>				
		a=2.0	a=2.5	<b>a=2.8</b>	a=3.0	a=3.5	a=2.0	a=2.5	<b>a=2.8</b>	a=3.0	a=3.5
EBF	-0.19	-0.16	-0.19	<b>-0.22</b>	-0.23	-0.27	0.82	1.02	<b>1.14</b>	1.21	1.40
NF	-0.23	-0.24	-0.29	<b>-0.33</b>	-0.35	-0.40	1.04	1.28	<b>1.43</b>	1.51	1.73
DBF	-0.70	-0.51	-0.63	<b>-0.70</b>	-0.74	-0.86	0.73	0.90	<b>1.00</b>	1.06	1.23
C_SHR	/	-1.22	-1.51	<b>-1.69</b>	-1.79	-2.07	/	/	/	/	/
A_SHR	/	-0.36	-0.45	<b>-0.50</b>	-0.53	-0.61	/	/	/	/	/
C4_GRA	-0.85	-0.79	-0.97	<b>-1.09</b>	-1.16	-1.34	0.92	1.15	<b>1.29</b>	1.36	1.58
C3_GR A	-0.62	-0.58	-0.72	<b>-0.80</b>	-0.85	-0.99	0.93	1.15	<b>1.30</b>	1.37	1.59
CRO	-3.35	-1.97	-2.67	<b>-3.17</b>	-3.46	-4.35	0.59	0.80	<b>0.94</b>	1.03	1.30
Fitting <sup>c</sup>	/	0.62	0.83	<b>0.98</b>	1.07	1.32	/	/	/	/	/
Median	/	/	/	/	/	/	0.87	1.08	<b>1.22</b>	1.29	1.49
Std	/	/	/	/	/	/	0.16	0.18	<b>0.19</b>	0.19	0.19

93

94 <sup>a</sup> All tests of the YIBs-LMA\_map experiment use the same threshold  $x=0.019$  nmol g<sup>-1</sup> s<sup>-1</sup> as YIBs-  
 95 LMA, but gridded LMA information from another LMA map of B2017. Details are summarized in  
 96 Table 1.

97 <sup>b</sup> Slopes of simulated PFT-specific DRR ( $S_S$ ) are divided by observations ( $S_O$ , Table S1) to derive  
 98 the model-to-observation ratios ( $S_S/S_O$ ). O<sub>3</sub> dose metric is POD<sub>y=1</sub> for natural PFTs and POD<sub>y=6</sub> for  
 99 crops. The Median and standard deviation (Std) of  $S_S/S_O$  ratios of all PFTs are calculated for each  
 100 setting of specific parameter  $a$ .

101 <sup>c</sup> The slopes (Fitting) of linear regressions between  $S_O$  and  $S_S$  are listed for each  $a$ . The optimal  $a$   
 102 with 1:1 fitting between  $S_S$  and  $S_O$  is bolded.

103



104 **Table S7.** PFT-specific  $a_{PFT}$  and  $y$  for YIBs-S2007\_adj<sup>a</sup> experiment.

105

PFT	EBF	NF	DBF	C_SHR <sup>c</sup>	A_SHR <sup>d</sup>	C4_GRA	C3_GRA	CRO
$a_{PFT}$ (nmol <sup>-1</sup> m <sup>2</sup> s)	0.023	0.017	0.042	0.015	0.030	0.041	0.041	0.039
$y$ (nmol m <sup>-2</sup> s <sup>-1</sup> ) <sup>b</sup>	1	1	1	1	1	1	1	1

106

107 <sup>a</sup> YIBs-S2007\_adj adopts area-based flux expression in S2007. The sensitivity parameter  $a_{PFT}$  are  
 108 recalibrated according to  $S_O$  in Table S1. Details are summarized in Table 1.

109 <sup>b</sup> The thresholds  $y$  are set to 1 nmol m<sup>-2</sup> s<sup>-1</sup> for all PFTs according to Oliver et al. (2018).

110 <sup>c</sup>  $S_O$  for calibrating C\_SHR is assumed as the mean of EBF and DBF in Table S1.

111 <sup>d</sup>  $S_O$  for calibrating A\_SHR is assumed as the mean of EBF and DBF in Table S1.

112

113 **Table S8.** Key parameters for the vegetation model. Maximum carboxylation capacity ( $\mu\text{mol m}^{-2}$   
 114  $\text{s}^{-1}$ ) at 25 degrees Celsius, leaf nitrogen content ( $\text{g m}^{-2}$ ).

<b>PFT</b>	<b>EBF</b>	<b>NF</b>	<b>DBF</b>	<b>C_SHB</b>	<b>A_SHB</b>	<b>C4_GRA</b>	<b>C3_GRA</b>	<b>CRO</b>
Vcmax25 ( $\mu\text{mol m}^{-2}$ $\text{s}^{-1}$ )	29.0	50.8	59.6	57.9	57.9	24.0	78.2	100.7
Nleaf ( $\text{g m}^{-2}$ )	2.17	2.46	1.80	1.86	1.86	1.32	1.75	1.62

115

116

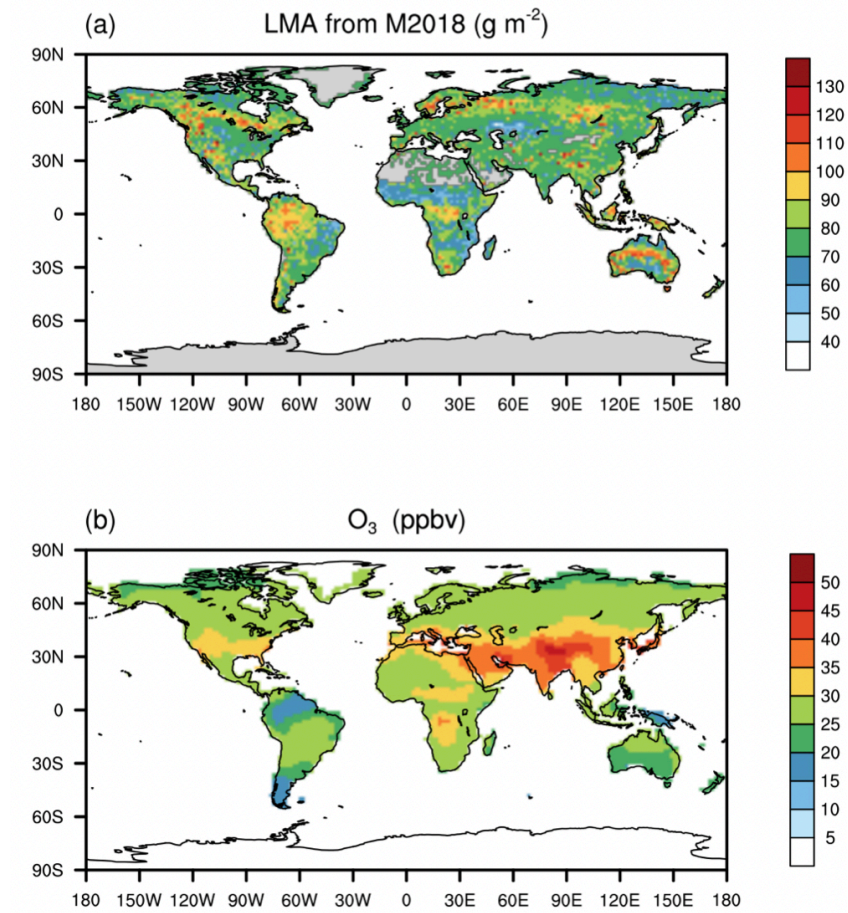
117 **Table S9.** Summary of O<sub>3</sub> vegetation damages. GPP of each PFT (GPP<sub>PFT</sub>, Pg C year<sup>-1</sup>), absolute  
 118 GPP changes of each PFT ( $\Delta$ GPP<sub>PFT</sub>, Pg C year<sup>-1</sup>), relative GPP changes of each PFT  
 119 ( $\Delta$ GPP<sub>PFT</sub>/GPP<sub>PFT</sub>, %), ratio of PFT-level GPP changes to global GPP ( $\Delta$ GPP<sub>PFT</sub>/GPP, %).

Simulations <sup>a</sup>		EBF	ENF	DBF	C_SHR	A_SHR	CRA_C4	GRA_C3	CRO	Total
No O <sub>3</sub>	GPP <sub>PFT</sub>	29.72	19.04	8.96	4.02	21.57	20.84	25.92	17.60	147.65
YIBs-LMA	GPP <sub>PFT</sub>	29.40	18.61	8.48	3.95	20.63	20.05	24.03	15.39	140.54
	$\Delta$ GPP <sub>PFT</sub>	-0.31	-0.43	-0.47	-0.07	-0.93	-0.79	-1.89	-2.21	-7.11
	$\Delta$ GPP <sub>PFT</sub> /GPP <sub>PFT</sub>	-1.05	-2.25	-5.27	-1.86	-4.33	-3.79	-7.28	-12.56	\
	$\Delta$ GPP <sub>PFT</sub> /GPP	-0.21	-0.29	-0.32	-0.05	-0.63	-0.53	-1.28	-1.50	-4.81
YIBs-LMA_PFT	GPP <sub>PFT</sub>	29.48	18.97	8.45	3.96	20.89	19.96	23.85	15.23	140.79
	$\Delta$ GPP <sub>PFT</sub>	-0.24	-0.07	-0.50	-0.06	-0.68	-0.89	-2.07	-2.37	-6.86
	$\Delta$ GPP <sub>PFT</sub> /GPP <sub>PFT</sub>	-0.80	-0.36	-5.61	-1.45	-3.13	-4.25	-7.98	-13.45	\
	$\Delta$ GPP <sub>PFT</sub> /GPP	-0.16	-0.05	-0.34	-0.04	-0.46	-0.60	-1.40	-1.60	-4.65
YIBs-LMA_T	GPP <sub>PFT</sub>	28.95	18.32	8.33	3.86	20.26	19.62	23.62	15.13	138.08
	$\Delta$ GPP <sub>PFT</sub>	-0.76	-0.72	-0.63	-0.16	-1.31	-1.22	-2.29	-2.47	-9.56
	$\Delta$ GPP <sub>PFT</sub> /GPP <sub>PFT</sub>	-2.57	-3.80	-7.00	-3.88	-6.08	-5.85	-8.85	-14.03	\
	$\Delta$ GPP <sub>PFT</sub> /GPP	-0.52	-0.49	-0.42	-0.11	-0.89	-0.83	-1.55	-1.67	-6.48
YIBs-LMA_B2017	GPP <sub>PFT</sub>	29.28	18.60	8.46	3.88	20.62	19.97	23.76	15.27	139.85
	$\Delta$ GPP <sub>PFT</sub>	-0.44	-0.44	-0.49	-0.14	-0.94	-0.87	-2.15	-2.32	-7.80
	$\Delta$ GPP <sub>PFT</sub> /GPP <sub>PFT</sub>	-1.47	-2.30	-5.52	-3.45	-4.38	-4.18	-8.31	-13.19	\
	$\Delta$ GPP <sub>PFT</sub> /GPP	-0.30	-0.30	-0.33	-0.09	-0.64	-0.59	-1.46	-1.57	-5.28
YIBs-S2007_adj	GPP <sub>PFT</sub>	29.32	18.75	8.39	3.98	20.76	20.02	23.95	15.41	140.58
	$\Delta$ GPP <sub>PFT</sub>	-0.39	-0.29	-0.56	-0.04	-0.81	-0.82	-1.97	-2.19	-7.07
	$\Delta$ GPP <sub>PFT</sub> /GPP <sub>PFT</sub>	-1.32	-1.53	-6.28	-1.02	-3.75	-3.92	-7.60	-12.44	\
	$\Delta$ GPP <sub>PFT</sub> /GPP	-0.27	-0.20	-0.38	-0.03	-0.55	-0.55	-1.33	-1.48	-4.79

120

121 <sup>a</sup> All results utilize optimal parameters shown in Table 1.

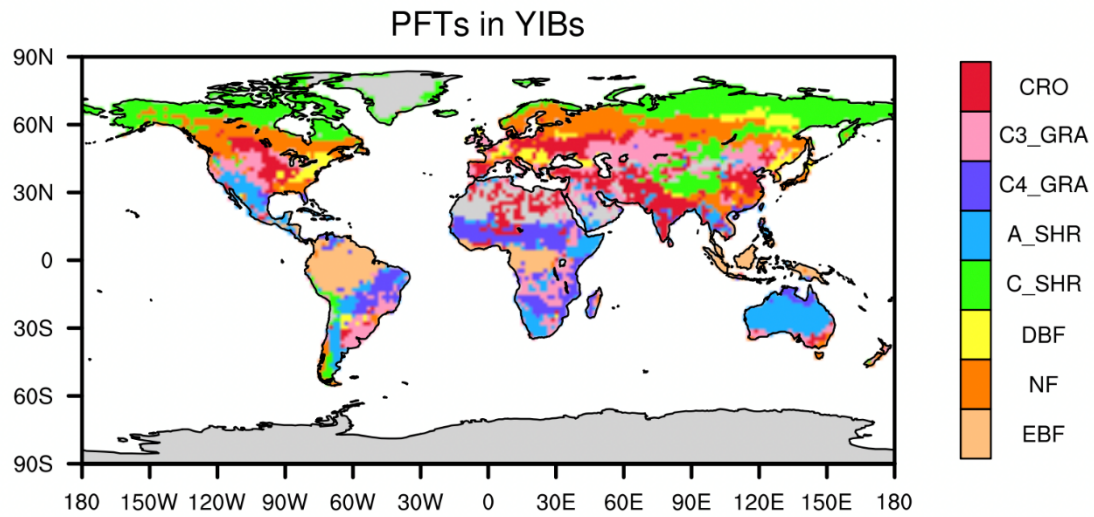
122



123

124 **Figure S1.** Global leaf mass per area (LMA) and surface ozone (O<sub>3</sub>) concentrations. The (a) LMA  
 125 is adopted from Moreno-Martinez et al. (2018) (M2018) and (b) annual mean O<sub>3</sub> is derived from  
 126 TF-HTAP(Turnock et al., 2018).

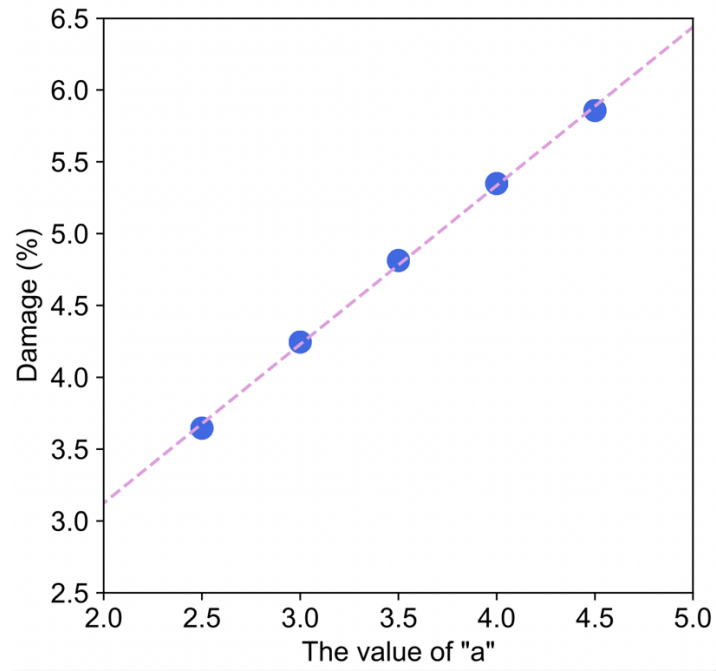
127



128

129 **Figure S2.** Dominant plant functional types (PFTs) in YIBs model. The PFTs include evergreen  
 130 broadleaf forest (EBF), needleleaf forest (NF), deciduous broadleaf forest (DBF), arid/cold  
 131 shrubland (A\_SHR/C\_SHR), C<sub>3</sub>/C<sub>4</sub> grassland (C<sub>3</sub>\_GRA/C<sub>4</sub>\_GRA), and cropland (CRO).

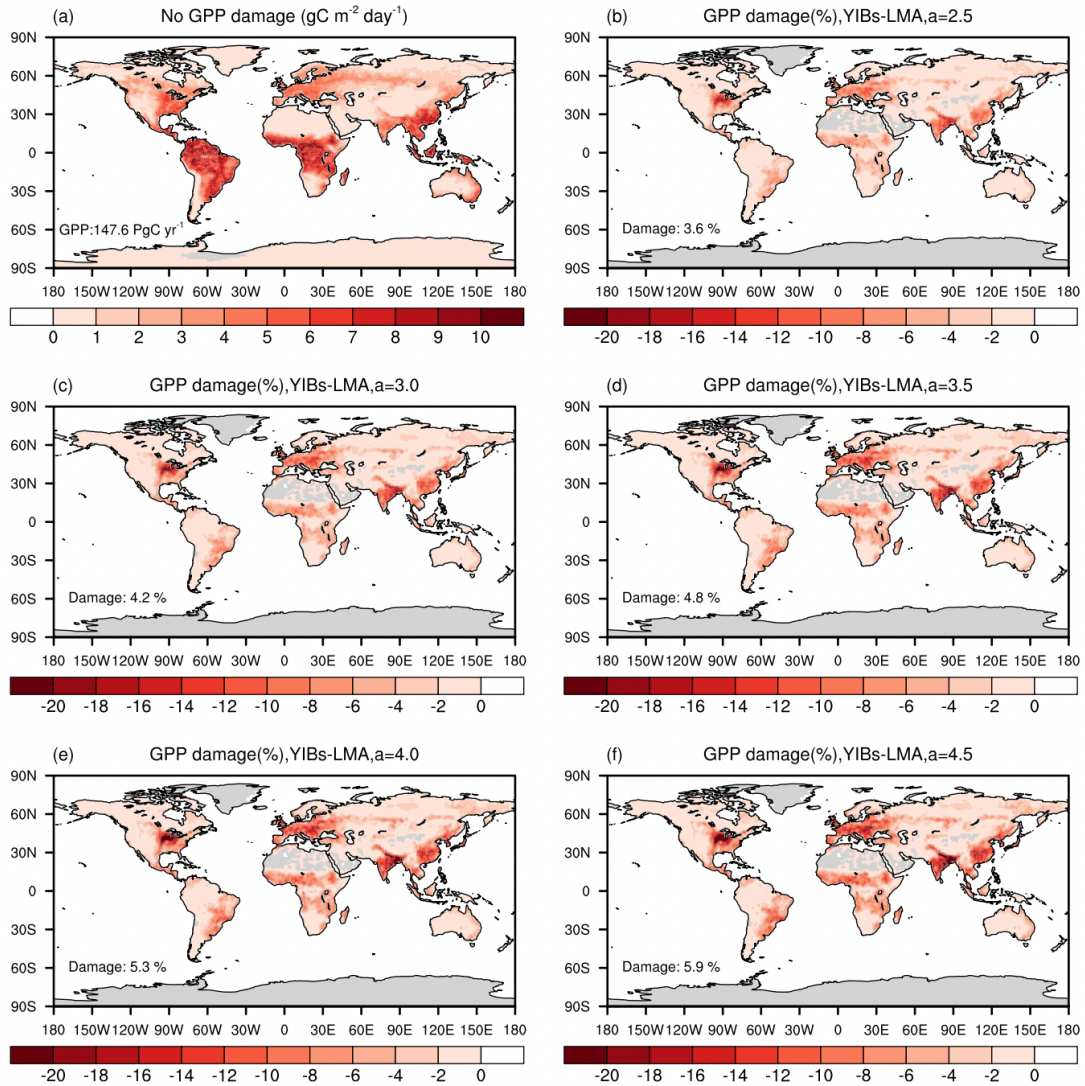
132



133

134 **Figure S3.** Derived O<sub>3</sub> damage percentages of global GPP (Damage, %) with varied parameter  $a$   
135 for the YIBs-LMA experiment. The YIBs-LMA experiment is described in Section 2.3 and Table 1.

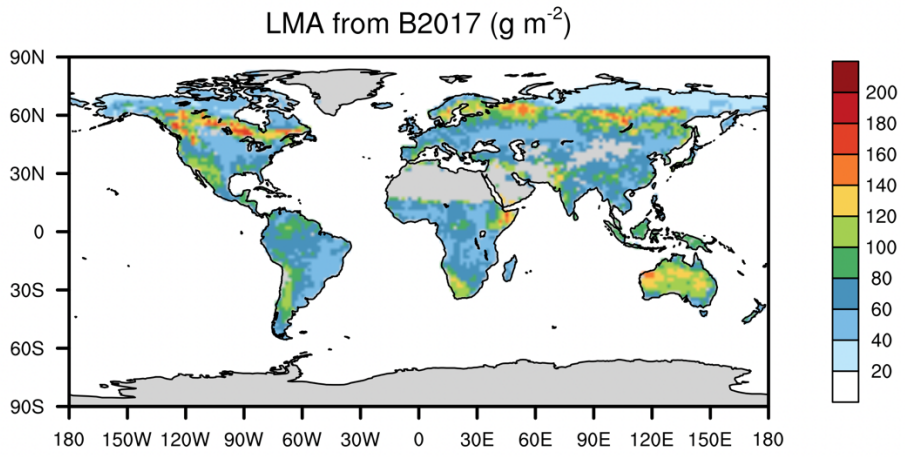
136



137

138 **Figure S4.** Global distribution of (a) GPP and (b-f) its damage percentages by  $\text{O}_3$  with different  
 139 parameter  $a$  for the YIBs-LMA experiment. The global total GPP is shown in (a) and the average  
 140 damage percentages are shown in (b-f). The YIBs-LMA experiment is described in Table 1.

141

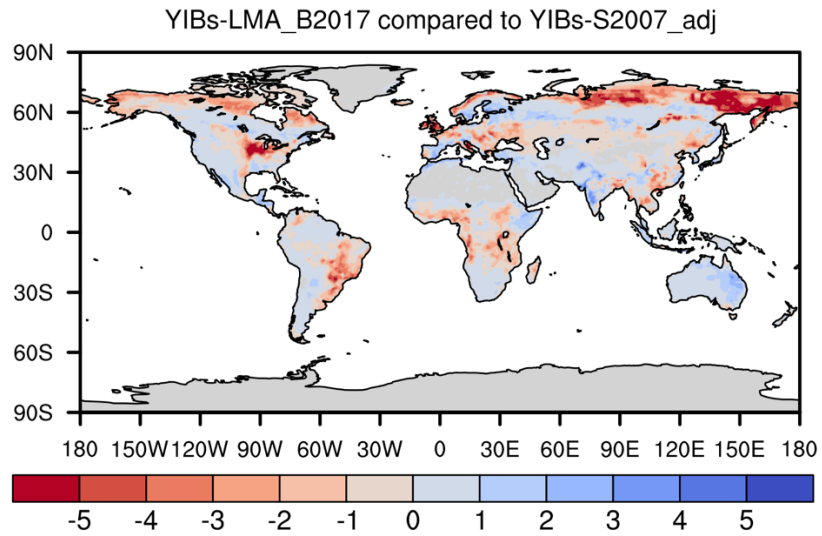


142

143 **Figure S5.** Distribution of LMA from B2017.

144





145

146 **Figure S6.** Differences between global O<sub>3</sub> vegetation damage map from the YIBs-LMA\_B2017  
 147 experiment with optimal  $a=2.8 \text{ nmol}^{-1} \text{ s g}$  and YIBs-S2007\_adj. Blue (red) patches indicate the  
 148 regions where damage in YIBs-LMA\_B2017 with optimal  $a$  are weaker (stronger) than YIBs-  
 149 S2007\_adj. Experiments are described in Table 1.

150

151 **Supplementary References**

- 152 Alonso, R., Elvira, S., Inclan, R., and Bermejo, V.: Responses of Aleppo pine to ozone, in: Dev Environm  
153 Sci, Developments in Environmental Science, 211-230, 2003.
- 154 Alonso, R., Elvira, S., Gonzalez-Fernandez, I., Calvete, H., Garcia-Gomez, H., and Bermejo, V.: Drought  
155 stress does not protect *Quercus ilex* L. from ozone effects: results from a comparative study of two  
156 subspecies differing in ozone sensitivity, *Plant Biology*, 16, 375-384, 10.1111/plb.12073, 2014.
- 157 Assis, P. I. L. S., Alonso, R., Meirelles, S. T., and Moraes, R. M.: DO3SE model applicability and O-3  
158 flux performance compared to AOT40 for an O-3-sensitive tropical tree species (*Psidium guajava* L.  
159 'Paluma'), *Environ Sci Pollut R*, 22, 10873-10881, 10.1007/s11356-015-4293-1, 2015.
- 160 Braun, S. and Fluckiger, W.: EFFECTS OF AMBIENT OZONE ON SEEDLINGS OF FAGUS-  
161 SYLVATICA L AND PICEA-ABIES (L) KARST, *New Phytol*, 129, 33-44, 10.1111/j.1469-  
162 8137.1995.tb03007.x, 1995.
- 163 Buker, P., Feng, Z., Uddling, J., Briolat, A., Alonso, R., Braun, S., Elvira, S., Gerosa, G., Karlsson, P. E.,  
164 Le Thiec, D., Marzuoli, R., Mills, G., Oksanen, E., Wieser, G., Wilkinson, M., and Emberson, L. D.:  
165 New flux based dose-response relationships for ozone for European forest tree species, *Environ Pollut*,  
166 206, 163-174, 10.1016/j.envpol.2015.06.033, 2015.
- 167 Calatayud, V., Cervero, J., Calvo, E., Garcia-Breijo, F.-J., Reig-Arminana, J., and Jose Sanz, M.:  
168 Responses of evergreen and deciduous *Quercus* species to enhanced ozone levels, *Environ Pollut*,  
169 159, 55-63, 10.1016/j.envpol.2010.09.024, 2011.
- 170 CLRTAP: The UNECE Convention on Long-range Transboundary Air Pollution, Manual on  
171 Methodologies and Criteria for Modelling and Mapping Critical Loads and Levels and Air Pollution  
172 Effects, Risks and Trends: Chapter III Mapping Critical Levels for Vegetation, 2017.
- 173 Dixon, M., Le Thiec, D., and Garrec, J. P.: Reactions of Norway spruce and beech trees to 2 years of  
174 ozone exposure and episodic drought, *Environ Exp Bot*, 40, 77-91, 10.1016/s0098-8472(98)00023-  
175 9, 1998.
- 176 Elvira, S., Alonso, R., and Gimeno, B. S.: Simulation of stomatal conductance for Aleppo pine to estimate  
177 its ozone uptake, *Environ Pollut*, 146, 617-623, 10.1016/j.envpol.2006.08.008, 2007.
- 178 Feng, Z. Z., Buker, P., Pleijel, H., Emberson, L., Karlsson, P. E., and Uddling, J.: A unifying explanation  
179 for variation in ozone sensitivity among woody plants, *Global Change Biol*, 24, 78-84,  
180 10.1111/gcb.13824, 2018.
- 181 Gimeno, B. S., Bermejo, V., Sanz, J., de la Torre, D., and Elvira, S.: Growth response to ozone of annual  
182 species from Mediterranean pastures, *Environ Pollut*, 132, 297-306, 10.1016/j.envpol.2004.04.022,  
183 2004a.
- 184 Gimeno, B. S., Bermejo, V., Sanz, J., De la Torre, D., and Gil, J. M.: Assessment of the effects of ozone  
185 exposure and plant competition on the reproductive ability of three therophytic clover species from  
186 Iberian pastures, *Atmos Environ*, 38, 2295-2303, 10.1016/j.atmosenv.2003.10.062, 2004b.
- 187 Harmens, H., Hayes, F., Mills, G., Sharps, K., Osborne, S., and Pleijel, H.: Wheat yield responses to  
188 stomatal uptake of ozone: Peak vs rising background ozone conditions, *Atmos Environ*, 173, 1-5,  
189 2018.
- 190 Hayes, F., Williamson, J., and Mills, G.: Ozone pollution affects flower numbers and timing in a  
191 simulated BAP priority calcareous grassland community, *Environ Pollut*, 163, 40-47,  
192 10.1016/j.envpol.2011.12.032, 2012.
- 193 Hayes, F., Harmens, H., Sharps, K., and Radbourne, A.: Ozone dose-response relationships for tropical  
194 crops reveal potential threat to legume and wheat production, but not to millets, *Scientific African*, 9,

195 2020.

196 Hayes, F., Mills, G., Harmens, H., and Wyness, K.: Within season and carry-over effects following  
 197 exposure of grassland species mixtures to increasing background ozone, *Environ Pollut*, 159, 2420-  
 198 2426, 10.1016/j.envpol.2011.06.034, 2011.

199 Hewitt, D. K. L., Mills, G., Hayes, F., Wilkinson, S., and Davies, W.: Highlighting the threat from current  
 200 and near-future ozone pollution to clover in pasture, *Environ Pollut*, 189, 111-117,  
 201 10.1016/j.envpol.2014.02.033, 2014.

202 Hoshika, Y., Moura, B., and Paoletti, E.: Ozone risk assessment in three oak species as affected by soil  
 203 water availability, *Environ Sci Pollut R*, 25, 8125-8136, 2018.

204 Hu, E., Gao, F., Xin, Y., Jia, H., Li, K., Hu, J., and Feng, Z.: Concentration- and flux-based ozone dose-  
 205 response relationships for five poplar clones grown in North China, *Environ Pollut*, 207, 21-30,  
 206 <https://doi.org/10.1016/j.envpol.2015.08.034>, 2015.

207 Karlsson, P. E., Uddling, J., Skarby, L., Wallin, G., and Sellden, G.: Impact of ozone on the growth of  
 208 birch (*Betula pendula*) saplings, *Environ Pollut*, 124, 485-495, 10.1016/s0269-7491(03)00010-1,  
 209 2003.

210 Karlsson, P. E., Uddling, J., Braun, S., Broadmeadow, M., Elvira, S., Gimeno, B. S., Le Thiec, D.,  
 211 Oksanen, E., Vandermeiren, K., Wilkinson, M., and Emberson, L.: New critical levels for ozone  
 212 effects on young trees based on AOT40 and simulated cumulative leaf uptake of ozone, *Atmos*  
 213 *Environ*, 38, 2283-2294, 10.1016/j.atmosenv.2004.01.027, 2004.

214 Marzuoli, R., Monga, R., Finco, A., and Gerosa, G.: Biomass and physiological responses of *Quercus*  
 215 *robur* (L.) young trees during 2 years of treatments with different levels of ozone and nitrogen wet  
 216 deposition, *Trees-Struct Funct*, 30, 1995-2010, 10.1007/s00468-016-1427-0, 2016.

217 Marzuoli, R., Bussotti, F., Calatayud, V., Calvo, E., Alonso, R., Bermejo, V., Pollastrini, M., Monga, R.,  
 218 and Gerosa, G.: Dose-response relationships for ozone effect on the growth of deciduous broadleaf  
 219 oaks in mediterranean environment, *Atmos Environ*, 190, 331-341, 10.1016/j.atmosenv.2018.07.053,  
 220 2018.

221 Medlyn, B. E., Badeck, F. W., De Pury, D. G. G., Barton, C. V. M., Broadmeadow, M., Ceulemans, R.,  
 222 De Angelis, P., Forstreuter, M., Jach, M. E., Kellomaki, S., Laitat, E., Marek, M., Philippot, S., Rey,  
 223 A., Strassmeyer, J., Laitinen, K., Liozon, R., Portier, B., Roberntz, P., Wang, K., and Jarvis, P. G.:  
 224 Effects of elevated CO<sub>2</sub> on photosynthesis in European forest species: a meta-analysis of model  
 225 parameters, *Plant Cell Environ*, 22, 1475-1495, 10.1046/j.1365-3040.1999.00523.x, 1999.

226 Moreno-Martinez, A., Camps-Valls, G., Kattge, J., Robinson, N., Reichstein, M., van Bodegom, P.,  
 227 Kramer, K., Cornelissen, J. H. C., Reich, P., Bahn, M., Niinemets, U., Penuelas, J., Craine, J. M.,  
 228 Cerabolini, B. E. L., Minden, V., Laughlin, D. C., Sack, L., Allred, B., Baraloto, C., Byun, C.,  
 229 Soudzilovskaia, N. A., and Running, S. W.: A methodology to derive global maps of leaf traits using  
 230 remote sensing and climate data, *Remote Sens Environ*, 218, 69-88, 2018.

231 Oliver, R. J., Mercado, L. M., Sitch, S., Simpson, D., Medlyn, B. E., Lin, Y. S., and Folberth, G. A.: Large  
 232 but decreasing effect of ozone on the European carbon sink, *Biogeosciences*, 15, 4245-4269,  
 233 10.5194/bg-15-4245-2018, 2018.

234 Ottosson, S., Wallin, G., Skarby, L., Karlsson, P. E., Medin, E. L., Rantfors, M., Pleijel, H., and Sellden,  
 235 G.: Four years of ozone exposure at high or low phosphorus reduced biomass in Norway spruce,  
 236 *Trees-Struct Funct*, 17, 299-307, 10.1007/s00468-002-0239-6, 2003.

237 Peng, J., Shang, B., Xu, Y., Feng, Z., and Calatayud, V.: Effects of ozone on maize (*Zea mays* L.)  
 238 photosynthetic physiology, biomass and yield components based on exposure- and flux-response

239 relationships, *Environ Pollut*, 256, 10.1016/j.envpol.2019.113466, 2020.

240 Peng, J. L., Shang, B., Xu, Y. S., Feng, Z. Z., Pleijel, H., and Calatayud, V.: Ozone exposure- and flux-  
241 yield response relationships for maize, *Environ Pollut*, 252, 1-7, 2019.

242 Sanz, J., Bermejo, V., Gimeno, B. S., Elvira, S., and Alonso, R.: Ozone sensitivity of the Mediterranean  
243 terophyte *Trifolium striatum* is modulated by soil nitrogen content, *Atmos Environ*, 41, 8952-8962,  
244 10.1016/j.atmosenv.2007.08.016, 2007.

245 Sanz, J., Muntifering, R. B., Bermejo, V., Gimeno, B. S., and Elvira, S.: Ozone and increased nitrogen  
246 supply effects on the yield and nutritive quality of *Trifolium subterraneum*, *Atmos Environ*, 39, 5899-  
247 5907, 10.1016/j.atmosenv.2005.06.022, 2005.

248 Sanz, J., Gonzalez-Fernandez, I., Elvira, S., Muntifering, R., Alonso, R., and Bermejo-Bermejo, V.:  
249 Setting ozone critical levels for annual Mediterranean pasture species: Combined analysis of open-  
250 top chamber experiments, *Sci Total Environ*, 571, 670-679, 10.1016/j.scitotenv.2016.07.035, 2016.

251 Sanz, J., Gonzalez-Fernandez, I., Calvete-Sogo, H., Lin, J. S., Alonso, R., Muntifering, R., and Bermejo,  
252 V.: Ozone and nitrogen effects on yield and nutritive quality of the annual legume *Trifolium cherleri*,  
253 *Atmos Environ*, 94, 765-772, 10.1016/j.atmosenv.2014.06.001, 2014.

254 Turnock, S. T., Wild, O., Dentener, F. J., Davila, Y., Emmons, L. K., Flemming, J., Folberth, G. A., Henze,  
255 D. K., Jonson, J. E., Keating, T. J., Kengo, S., Lin, M., Lund, M., Tilmes, S., and O'Connor, F. M.:  
256 The impact of future emission policies on tropospheric ozone using a parameterised approach, *Atmos*  
257 *Chem Phys*, 18, 8953-8978, 10.5194/acp-18-8953-2018, 2018.

258 Uddling, J., Pleijel, H., and Karlsson, P. E.: Measuring and modelling leaf diffusive conductance in  
259 juvenile silver birch, *Betula pendula*, *Trees-Struct Funct*, 18, 686-695, 2004.

260 Wagg, S., Mills, G., Hayes, F., Wilkinson, S., Cooper, D., and Davies, W. J.: Reduced soil water  
261 availability did not protect two competing grassland species from the negative effects of increasing  
262 background ozone, *Environ Pollut*, 165, 91-99, 10.1016/j.envpol.2012.02.010, 2012.

263 Wyness, K., Mills, G., Jones, L., Barnes, J. D., and Jones, D. L.: Enhanced nitrogen deposition  
264 exacerbates the negative effect of increasing background ozone in *Dactylis glomerata*, but not  
265 *Ranunculus acris*, *Environ Pollut*, 159, 2493-2499, 10.1016/j.envpol.2011.06.022, 2011.

266 Zhang, W. W., Feng, Z. Z., Wang, X. K., Liu, X. B., and Hu, E. Z.: Quantification of ozone exposure-  
267 and stomatal uptake-yield response relationships for soybean in Northeast China, *Sci Total Environ*,  
268 599, 710-720, 10.1016/j.scitotenv.2017.04.231, 2017.

269